Archives of Hydro-Engineering and Environmental Mechanics
Vol. 60 (2013), No. 1–4, pp. 31–50
DOI: 10.2478/heem-2013-0000-7

VERSITA

Lagrangian Model for a Single Saltating Grain in the Near-Wall Region of an Open-Channel Flow

Włodzimierz Czernuszenko

Institute of Geophysics, Polish Academy of Sciences, 01-452 Warszawa, Ks. Janusza 64, Poland,
e-mail: wczer@igf.edu.pl

(Received July 06, 2012; revised October 04, 2012)

Abstract

A mathematical model for the continuous saltation of a particle near the granular bed in an open-channel flow is developed in detail. The model is based on the Lagrangian equations governing particle motion, and it takes into account the following forces: drag, lift, gravitation, virtual mass and the force responsible for particle-particle interactions. A model of particle-particle collisions is developed and used to determine the mean impulsive force acting upon a particle flowing and rebounding from the channel bed. The model can simulate the continuous saltation trajectories of a single particle in the near-bed region of turbulent flows, in which particle motion is controlled by collisions. The model has been calibrated and verified with available published data in a rather wide range of grain sizes from 0.53 mm to 15 mm. All parameters, such as lift, drag, restitution, friction coefficients and roughness height, have been set on the basis of a reanalysis of these published data.

Key words: Lagrangian model, open-channel flow, particle-particle interaction

Notation

A_D – cross-sectional area of the grain,
$a_D = A_D D/V$ and $a_L = A_L D/V$ – (for spherical particles these coefficients are equal to 3/2),
C_D – drag coefficient,
C_L – lift coefficient,
C_m – virtual mass coefficient,
D – particle size (diameter),
$\mathbf{e}_D, \mathbf{e}_L$ – unit vectors in the directions of the drag and lift forces, respectively,
F – inertia force,
F_a – added force,
F_D – drag force,
F_g – gravitational force,
F_L – lift force,

g – gravitational acceleration,
H – water depth,
H_S – saltation height,
$\mathbf{I}$ – second order identity tensor,
$\mathbf{J}$ – impulsive force exerted on particle 1,
k_e – effective size of roughness interfering with the flow,
$\mathbf{n}$ – unit vector normal to the surface of the grain,
p – pressure,
p_o – pressures along the stagnation streamline at the upstream-infinity,
Re – Reynolds number,
R_r – roughness Reynolds number,
T – time,
T_s – travel time of a single step during the saltating particle,
$\mathbf{U}$ – mean velocity,
$\mathbf{U}_*$ – friction velocity,
$\mathbf{U}_{*c}$ – critical friction velocity,
$\mathbf{u}_r = \mathbf{u}_f - \mathbf{u}_s$ – particle slip velocity,
V – volume of the grain,
$\mathbf{V}^0$ and $\mathbf{V}$ – relative velocities between particles before and after collision,
α – collision angle,
Θ – angle between the vector normal to the surface of the grain, n, and $\mathbf{e}_x$,
θ_{in} – incidence (impact) angles (see Fig. 2),
ν – kinematic viscosity,
ρ – density of the fluid (water),
ρ_s – density of the sediment,
$\tau_\mathbf{b}$ or $\tau_\mathbf{o}$ – bed shear stress,
$\tau_\mathbf{c}$ – critical shear stress,
τ_{up} and τ_{dw} – mean free time when the particle moves upward and downward, respectively,
Φ – channel-bed angle.

Subscripts

f – fluid phase,
s – sediment phase,
1 and 2 – refer to the velocity of two particles,

Superscript

0 – means values before collision.

1. Introduction

Bed load sediment can be transported in several ways. A grain begins to move by rolling over the surface of the bed, but with a small increase in boundary shear stress this grain hops up from the bed and follows ballistic-like trajectories. This motion is called saltation, and it is considered as the dominant mode of bed-load transport (Sekine and Kikkawa 1992). Bagnold (1956) describes saltation as the unsuspended transport of particles over a granular bed by a fluid flow, in the form of consecutive hops within the near-bed region. It is governed mainly by the action of hydrodynamic forces that carry particles through the flow.

Using a computational hydrodynamic/sediment transport model involves a numerical solution of one or more of the governing differential equations of continuity, momentum and energy of the fluid, along with the differential equation for sediment continuity. There is one objection to using this kind of models. The transport of sediment takes place in a thin layer of mutual interaction between the erode-mobility bed and the fluid. The movement of the fluid and particles of sediment in this layer is very complicated, and therefore it is useless to apply typical governing equations. Nowadays, it is believed that one good approach to describing the movement of a single particle in the fluid is based on the analysis of [lub "to analyse"] all forces acting on the particle.

A number of researchers have worked on the modeling of grain saltation in flowing water, e.g. van Rijn (1987), Wiberg and Smith (1985), Sekine and Kikkawa (1992), Nino and Garcia (1996). Some of their studies concern the saltation of gravel and some others the saltation of sand. The behavior of discrete particles (sand grains) in the near-bed region of turbulent flows is considered under equilibrium conditions, i.e. particles of sand grains are carried by the flow without net erosion and deposition. All these models are based on the Lagrangian equation governing particle motion and on deterministic or stochastic approaches for estimating the initial conditions. This equation is written according to Newton's second law, i.e. the rate of change of the momentum of the particle is balanced against the surface and body forces acting on it.

Recently, Bialik (2011) has introduced a new concept of collision between flowing particles based on the statistical theory of gases. He assumes the possibility of three-way collisions between two particles. The model becomes more complicated, but he shows that it takes into account all possible collisions.

A particle trajectory in a turbulent flow in an open-channel depends largely on the concentration of particles. At great particle concentrations there is an interaction between particles through collisions, and the resulting force is significant in the balance of all forces exerted on the particle. Herein, a model for gravel saltation is proposed. The model includes all forces exerted on the moving particle in turbulent flows in the vicinity of the bed. They are steady-state drag forces, pressure gradient and buoyancy forces, unsteady forces (virtual mass and Basset forces), lift forces (Saffman and Mag-

nus forces) and some body forces as well as the collision force. Particles are assumed to be uniform in both shape and size. A series of sensitivity analyses is performed for various flow conditions, and the influence of particular forces during the whole course of a single hop is investigated.

2. Basic Equations

To describe the trajectory of a sediment grain (particle) in flowing water, the equation of motion for the particle is considered:

$$m_s \frac{d\mathbf{u_s}}{dt} = -m_s \mathbf{g} - \int_S (p\,\mathbf{n}\cdot\mathbf{I} - \mathbf{n}\cdot\tau)\; dS, \tag{1}$$

where ρ_s is the grain density, $\mathbf{u}_s$ is the grain velocity, g is the gravitational acceleration, p is the pressure, $\mathbf{n}$ is a unit vector normal to the surface of the grain, $\mathbf{I}$ is the second order identity tensor,and τ is the shear stress tensor.

The expression in brackets represents the total surface forces acting on the grain (particle). It is the sum of the pressure and shear stress. Usually, the magnitude of the pressure is much larger than that of the viscous stress, and the latter is negligible in problems of sediment hydraulics (see Wiberg and Smith 1985).

The pressure term can be found from the Navier-Stokes equation for water flow in the form

$$\frac{d\mathbf{u}_f}{dt} = -\frac{1}{\rho}\mathbf{grad}\,p + \nu\Delta^2\mathbf{u}_f - \mathbf{g}, \tag{2}$$

where ρ is the fluid density, $\mathbf{u}_f$ is the fluid velocity, ν is the kinematics viscosity and $\mathbf{g}$ is the gravitational acceleration.

To find the pressure, one is limited to steady and non-viscous flows, for which the equation Eq.(2) after integration becomes

$$\rho g z + p + \frac{1}{2}\rho u^2 = \text{const.} \tag{3}$$

Eq. (3) is called the Bernoulli equation, and it is valid along a streamline, i.e. each term varies from one streamline to another over the cross section. Usually, in an open-channel flow the free surface coincides with the hydraulic grade line and is very small. Then z is the height of the bed about datum, p/ρg can be treated as the vertical distance from the bed to the water surface, and (const/ρg) as the total energy head.

Writing Eq. (3) for the stagnation streamline and omitting the bed slope, one can obtain

$$p = p_o + \frac{1}{2}\rho\left(u_f^2 - u_s^2\right). \tag{4}$$

Eq.(4) is substituted into the pressure term of (1) to give the pressure force

$$\mathbf{F}_p = -\int_s p\mathbf{n}\cdot\mathbf{I}dS = -\int_s p_0 n\cdot\mathbf{I}dS - \int_s \frac{1}{2}\rho\left(u_f^2 - u_s^2\right)\mathbf{n}\cdot\mathbf{I}dS. \tag{5}$$

The first term on the right side of Eq. (5) corresponds to the pressure of the ambient flow. Using the Gauss divergence theorem and Eq. (2), it can be presented in the form

$$-\int_s p_0\mathbf{n}\cdot\mathbf{I}dS = -\int_V \Delta p_0 dV = m_f\frac{d\mathbf{u}_f}{dt} + m_f\mathbf{G}. \tag{6}$$

The above equation is related to the volume of the grain, V. The second term on the right side of (5) can be split into two orthogonal components that represent the drag and lift forces exerted by the fluid flowing around the grain, as displayed below:

$$\mathbf{F}_D = -\int_s \frac{\rho}{2}\left(u_r^2 - u_s^2\right)\mathbf{n}\cdot\mathbf{I}\cdot\mathbf{e}_D dS = -\int_s \frac{\rho}{2}\left(u_f^2 - u_s^2\right)\cos\theta dS, \tag{7}$$

$$\mathbf{F}_L = -\int_s \frac{\rho}{2}\left(u_r^2 - u_s^2\right)\mathbf{n}\cdot\mathbf{I}\cdot\mathbf{e}_L dS = -\int_s \frac{\rho}{2}\left(u_f^2 - u_s^2\right)\sin\theta dS, \tag{8}$$

where $\mathbf{e}_D$ and $\mathbf{e}_L$ are the unit vectors in the directions of the drag and lift forces, and Θ is the angle between a vector normal to the surface of the grain $\mathbf{n}$, and $\mathbf{e}_D$. The drag force acts in the direction of $(\mathbf{u}_f - \mathbf{u}_s)$, and thus it changes direction as the grain moves relative to the fluid.

Because the flow around spherical sediment particles is inviscid, integration over the surface of the grain in the above equation equals zero (D'Alembert paradox). To avoid this difficulty, the drag force can be written in terms of a fixed Cartesian coordinate system, as the dimensional analysis is used to find the form of true drag and lift forces in viscous flows (Wiberg and Smith 1985)

$$\mathbf{F}_D = C_D\frac{\rho A_D}{2}|u_r|(u_f - u_s,\ v_f - v_s), \tag{9}$$

$$\mathbf{F}_L = C_L A_L\frac{\rho}{2}\left[\left(u_r^2\right)_T - \left(u_r^2\right)_B\right]\mathbf{e}_e, \tag{10}$$

where in Eq. (9) C_D is the drag coefficient, A_D is the cross-sectional area of the grain, and in Eq. (10) C_L is the lift coefficient, A_L is the cross-sectional area of the grain in the plane normal to the lift force, $(u_r^2)_T$ and $(u_r^2)_B$ are velocities taken at the top and at the bottom of the particle, respectively. The drag force acts in the direction on the relative velocity according to Eq. (9), but the lift force in Eq. (10) is directed perpendicular to the direction of the fluid (see van Rijn 1987). Coleman (1967) shows that this formula works well for a sphere resting on a bed consisting of other spheres.

The lift force on sediment particles near the wall in a turbulent boundary layer is less well understood than the drag. Some authors, e.g. Willets and Naddech (1986),

dispute even the direction of the lift on particles near the bed. Eq. (10) suggests that the lift force ought to correlate with the velocity at the top of the particle because the velocity at the bottom will be much smaller. Schmeeckle et al (2007) show that the correlation is extremely weak. Hence the conclusion that the lift is impossible to compute in the same manner as the drag coefficient, and therefore it is not adequately predicted by Eq. (10). However, Wiberg and Smith (1985) used this equation and set the coefficient $C_L = 0.5$. The analysis of Auton et al (1987) for a spherical particle in a uniform flow gives $C_L = 1/3$.

There is an additional source for the lift force on a particle: the Magnus effect. This effect is the lift developed as a result of the rotation of the particle. The lift is caused by a pressure difference between both sides of the particle resulting from the velocity differential due to rotation. For saltation in water, it seems to be very small and will therefore be omitted in further analysis (see Wiberg and Smith 1985).

If the flow is unsteady, the force responsible for the relative acceleration of the body with respect to the surrounding fluid appears, and in addition to the real mass of the body it includes the virtual mass or added mass. The added mass is often called the virtual mass force F_a and usually described with the formula

$$\mathbf{F_a} = C_m V \rho \frac{\partial}{\partial t}\left(\mathbf{u}_f - \mathbf{u}_s\right), \tag{11}$$

where C_m is the virtual mass coefficient. For spheres in a weakly shearing flow it equals 0.5.

Some authors also discuss the Basset force that accounts for viscous effects due to acceleration. The value of the Basset force depends on the acceleration history up to the present time. This force is difficult to evaluate and usually negligible for a slow water velocity. Employing the relations for gravitational, pressure and added mass forces in Eq. (1), one can write

$$\begin{gathered} m_s \frac{d\mathbf{u_s}}{dt} = m_f \mathbf{g} + m_f \frac{d\mathbf{u}_f}{dt} + \rho \frac{C_D A_D}{2} u_r \mathbf{u}_r + m_f C_m \frac{\partial \mathbf{u_r}}{\partial t}, \\ \rho \frac{C_L A_L}{2} \left[\left(u_r^2\right)_T - \left(u_r^2\right)_B\right] \mathbf{e}_L - m_s \mathbf{g}, \end{gathered} \tag{12}$$

where $\mathbf{u}_r = \mathbf{u}_f - \mathbf{u}_s$ is the particle slip velocity, such that $\mathbf{u}_r = (u_f - u_s, -v_s)$.

Because the ambient flow is uniform, the partial derivative in the virtual mass term can be replaced by d/dt. After dividing the equation by V and introducing two factors $a_D = A_D D/V$ and $a_L = A_L D/V$ (for spherical particles these coefficients are equal to 3/2), one obtains

$$(\rho_s) \frac{d\mathbf{u}_s}{dt} = \rho \frac{d\mathbf{u_f}}{dt} - (\rho_s - \rho)\, \mathbf{g} + \rho \frac{C_D a_D}{2D} u_r \mathbf{u}_r + \rho C_m \frac{d\mathbf{u}_r}{dt} + \rho \frac{C_L a_L}{2D} \left[\left(u_r^2\right)_T - \left(u_r^2\right)_B\right] \mathbf{e}_L. \tag{13}$$

Velocities at the top and at the bottom of the hemisphere are given approximately by a log-law profile.

3. Log-Law Profile

The vertical velocity profile for a given roughness geometry and zero pressure gradient boundary-layer flows is Prandtl's log-law, usually presented in the following form:

$$\frac{U(y)}{U_*} = \frac{1}{\kappa} \ln \frac{y}{k_e} + B = \frac{1}{\kappa} \ln \frac{y}{y_0}, \tag{14}$$

where $U(y)$ is the time averaged velocity, U_* is the friction velocity, von Karman's constant κ is 0.41, k_e is the effective size of roughness interfering with the flow, y is the distance from the bed, and y_0 is the velocity origin.

The above equation is universal for zero pressure gradient boundary-layer flows. It is easy to see that the velocity origin is located over the theoretical (virtual) bed at $y_0 = k_e \exp(-\kappa B)$. The location of an origin vertical coordinate system is defined by the effective size of roughness elements. This location was determined by the Clauser method suggested by Perry at el. (1969). The coefficient B depends on the regime of turbulent flow, which is defined by a non-dimensional number ($U_* k/\nu$), but for the rough turbulent regime it can be taken as 5.3, Czernuszenko (2007).

4. Model of Particle-Particle Interaction

The movement of a sand grain in the bed vicinity is controlled by collisions with other moving grains or with grain comprises the bed. It will be assumed, that particles of sand have a spherical shape and constitute the dispersed phase, i.e. particles are not connected. Then it is possible to consider only simple binary collisions, not multiple collisions. Collisions take place in a very short time; hence all external forces can be neglected, and the impulse equations are considered in the following forms:

$$m_1(\mathbf{v}_1 - \mathbf{v}_1^0) = \mathbf{J}; \quad m_2(\mathbf{v}_2 - \mathbf{v}_2^0) = -\mathbf{J}, \tag{15}$$

where $\mathbf{J}$ is the impulsive force exerted on particle 1, the force $-\mathbf{J}$ acts on particle 2 as the reaction force, and n is the unit normal vector directed from particle 1 to particle 2 at the moment of contact (see Fig. 1). The subscripts 1 and 2 refer to the two particles, and the superscript 0 means values before collision.

The relative velocity vectors between particles before and after collision are

$$\mathbf{V}^0 = \mathbf{v}_1^0 - \mathbf{v}_2^0; \quad \mathbf{V} = \mathbf{v}_1 - \mathbf{v}_2. \tag{16}$$

The relationship between the pre-collision and post-collision velocities is obtained by using the coefficient of restitution. For spherical elements the restitution coefficient e is defined as the ratio of the pre- and post-collision velocities, that is

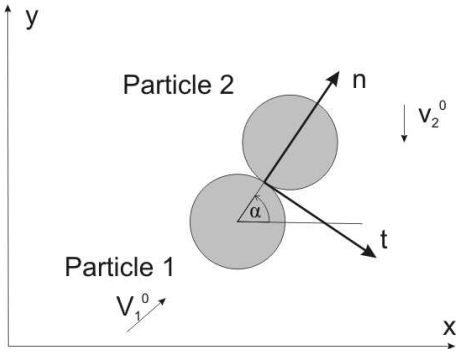

Fig. 1. Particle-particle collision. Spherical particles 1 and 2 with the same masses and sizes at the moment of collision; **n** and **t** are unit orthogonal vectors located at the point of contact; v_1^0 and v_2^0 are the initial velocities before collision

$$\mathbf{n} \bullet V = -e(\mathbf{n} \bullet V^0), \tag{17}$$

$\mathbf{n} \bullet V$ = dot product of vectors, n = unit normal vector from particle 1 to particle 2 at the point of contact, $\mathbf{V}^0$ and $\mathbf{V}$ = the relative velocities between particles before and after collision.

It is easy to obtain the relationship for post-collision velocities from Eqs. (15)–(17).

$$\mathbf{V} = \mathbf{V}^0 + \left[\frac{(m1 + m2)}{m1m2}\right]\mathbf{J}. \tag{18}$$

The normal component of the impulsive force J_n exerted on particle 1 is given as

$$J_n = -\left[\frac{m1m2}{(m1 + m2)}\right](1 + e)(\mathbf{n} \bullet \mathbf{V}^0), \tag{19}$$

Assuming that the particles slide during collision, the tangential component of the impulsive force from Coulomb's law for friction (Crowe et al 1998) is

$$J_t = fJ_n \text{ or in vector form } \mathbf{J}_t = fJ_n\mathbf{e}_t. \tag{20}$$

The absolute value of the impulse force in the $t - n$ plane $\mathbf{J} = (J_t, J_n)$ is

$$J = \sqrt{(J_n^2 + J_t^2)} = J_n\sqrt{(1 + f^2)}. \tag{21}$$

The components of the impulse force, in the $x - y$ plane are $\mathbf{J} = (J_x, J_y)$, where

$$J_x = (J_{t,x} + J_{n,x}) \text{ and } J_y = (J_{t,y} + J_{n,y}), \text{ for } f = 0, \quad J_x = J_{n,x} \text{ and } J_y = J_{n,y}. \tag{22}$$

Please, note that all the above equations are developed on the basis of two impulsive force equations without impulsive torque equations. It means that the rotations of colliding particles are not taken into account.

The role of the tangential component of the impulsive force in the process of collision is shown by comparison of the total impulsive force with and without friction during the collision of two particles (Fig. 2). The forces acting on spherical particles during their collision depend on the angle of collision. The components of these forces for collision without the friction force (J_{n_x}, J_{n_y}), and with friction ($J_{\_x}$, $J_{\_y}$) are shown in Figure 2 as a function of the collision angle. The maximum of the impulsive forces J_n between particles appears at $\alpha = 94.5°$ (this is the case in which the vectors $\mathbf{V}^\circ$ and $\mathbf{n}$ are parallel to each other). It is easy to notice that for $\alpha = 90°$ the horizontal component of the impulsive force $J_{n,x}$ changes its sign from negative to positive, but for collision with friction it happens at $\alpha = 50.6°$.

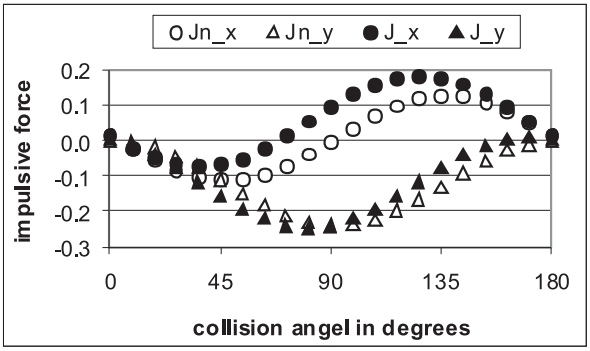

Fig. 2. The components of the total impulsive force (in $Ns \times 10^{-3}$) for collisions between two identical particles (D = 1.36 mm with masses of 0.00348 g) for the restitution friction coefficient $e = 1$ and the friction coefficient $f = 0.4$ [J_x, J_y] and without the friction force ($f = 0$) [Jn_x, Jn_y] as a function of different collision angles; pre-collision velocities are v_1^0 = (1.25 m/s, 0.485 m/s), v_2^0 = (1.30 m/s, –0.20 m/s)

5. Force Responsible for Collision

If the location of collision contact between particles is known, it is easy to define the force responsible for collision on the basis of the above equations. Usually, the location of the contact point is unknown, and even impossible to predict. Therefore, it is assumed that the location is a random function with a uniform probability distribution in the angle range from 0 to π. Then the mean impulsive force can be calculated without difficulty as

$$\overline{\mathbf{J}} = \frac{1}{\pi} \int_0^{\pi} \mathbf{J}\, da. \tag{23}$$

If there are more collisions, i.e., n collisions during the movement of the particle upward (force is directed downward) and the same in the opposite direction (force is

directed upward), then the mean force acting on a given particle during the whole hop of the particle $n(t_{up} + t_{dw})$ takes the following form:

$$\overline{\mathbf{F_{pc}}} = \begin{cases} -n\bar{\mathbf{J}}/t_{up} \text{ for time of particle movement upward} \\ n\bar{\mathbf{J}}/t_{dw} \text{ for time of particle movement downward,} \end{cases} \tag{24}$$

where t_{up} and t_{dw} are the mean free times when the particle moves upward and downward, respectively – it is assumed that they are equal to each other. [w opisie (16) proponuję: "for the time of the upward/downward movement"]

Table 1. The average components of the impulsive force (J_x, J_y) in g m/s – Eq. (15) – for collisions between two identical particles (D = 1.36 mm with masses of 0.00348 g) as a function of the restitution coefficient and the friction coefficient; pre-collision velocities are $v10$ = (1.25 m/s, 0.485 m/s), $v20$ = (1.30 m/s, –0.20 m/s). Note: All forces acting on particle 1 (flowing upward) are negative, i.e., acting against the movement of particle 1. All forces acting on particle 2 (flowing downward) are positive (see Eq. 16)

	f = 0.2	f = 0.2	f = 0.4	f = 0.4	f = 0.6	f = 0.6
e	J_x	J_y	J_x	J_y	J_x	J_y
1.0	0.373	0.402	0.28	0.469	0.187	0.536
0.2	0.224	0.241	0.168	0.282	0.112	0.322

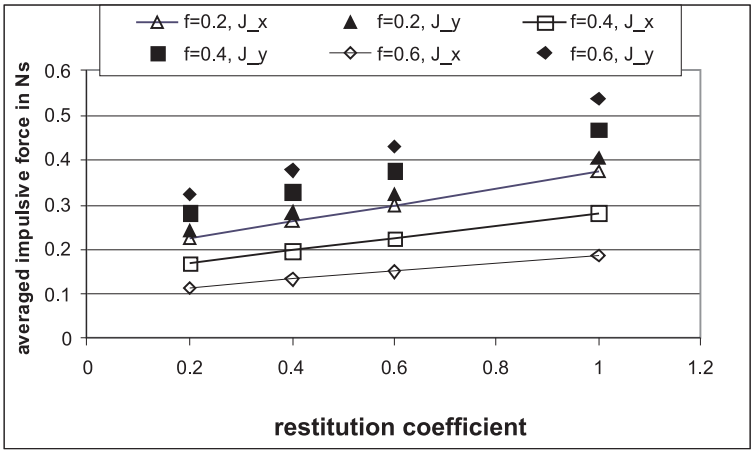

Fig. 3. The average impulsive force Eq. (15) for collisions between two identical particles (D = 1.36 mm with masses of 0.00348 g) as a function of the restitution coefficient and the friction coefficient; pre-collision velocities are v_1^0 = (1.25 m/s, 0.485 m/s), v_2^0 = (1.30 m/s, –0.20 m/s)

Figure 3 shows that for any value of the restitution coefficient, the impulsive force J_x increases when the friction coefficient decreases, and J_y increases when the friction coefficient increases (see Table 1).

Now, the equation describing the movement of a single sediment particle, i.e. Eq. (12), can be completed with the force responsible for particle-particle interaction, i.e. Eq. (16). It is worth mentioning that the direction of this force depends on the phase of the flowing particle [może "the flow direction"]. When the particle flows upward, the force is negative, and when it flows downward, the force is positive.

6. Equations for a Particle Saltating in Water

The slow motion of a spherical particle in a fluid may be described by Newton's equation (12) completed with the force $\mathbf{F}_{pc}$ exerted on the saltating particle by another particle during collision when the particle moves downward

$$\begin{gathered} m_s \frac{d\mathbf{u_s}}{dt} = m_f \mathbf{g} + m_f \frac{d\mathbf{u_f}}{dt} + \rho \frac{C_D A_D}{2} u_r \mathbf{u_r} + m_f C_m \frac{\partial \mathbf{u_r}}{\partial t}, \\ \rho \frac{C_L A_L}{2} \left[\left(u_r^2 \right)_T - \left(u_r^2 \right)_B \right] \mathbf{e}_L - m_s \mathbf{g} + \mathbf{J}/\tau, \end{gathered} \tag{25}$$

Finally, Eq. (17) can be re-write for the horizontal drag force in the following non-vector forms:

$$\frac{du_s}{dt} = \frac{3C_D \rho}{4D\left(\rho_s + C_m \rho\right)} \left| u_f - u_s \right| \left(u_f - u_s \right) - \frac{\rho_s - \rho}{\rho_s + \rho C_m} g_x + \frac{1}{\rho_s + C_m \rho} \frac{J_x}{\tau V}, \tag{26}$$

$$\begin{gathered} \frac{dv_s}{dt} = \frac{\rho}{\rho_s + \rho C_m} \frac{3C_D}{4D} \left(u_f - u_s \right) (-v_s) + \\ + \frac{\rho}{\rho_s + \rho C_m} \frac{3C_L}{4D} \left[\left((u_r)^2 \right)_T - \left((u_r)^2 \right)_B \right] \left(\frac{u_f - u_s}{|\mathbf{u_r}|} \right) - \frac{\rho_s - \rho}{\rho_s + \rho C_m} g_y + \frac{1}{\rho_s + \rho C_m} \frac{J_y}{\tau V}. \end{gathered} \tag{27}$$

Note that the force $\mathbf{J}$ is defined by Eqs. (19) and (20), i.e., $J_n = -\frac{m}{2}(1+e)\left(n \cdot V^0\right)$ and $J_t = f\, J_n$. Then the last term in above equation takes the following form:

$$\frac{1}{\rho_s + \rho C_m} \frac{J_y}{\tau V} = \frac{1}{\rho_s + \rho C_m} \frac{J_{n,y} + J_{t,y}}{\tau V} = \frac{1}{\rho_s + \rho C_m} \frac{m(1+e)(n \cdot V^0)_y}{2\tau V}, \tag{28}$$

where $\mathbf{g} = (g_x, g_y) = (g \sin \gamma\ , g \cos \gamma)$, and γ is the channel bed slope.

To find a trajectory of the saltating particle, the above set of equations is supplemented with the following Lagrangian equations:

$$\frac{dx}{dt} = u_s \text{ and} \frac{\mathrm{dy}}{\mathrm{dt}} = \mathrm{v_s}. \tag{29}$$

It is easy to get the balance all forces acting in the vertical direction

$$(\rho_s V)\frac{dv_s}{dt} = \rho V \frac{3C_D}{4D}\left(u_f - u_s\right)(-v_s) + \\ +\rho V \frac{3C_L}{4D}\left[\left(\left(u_f - u_s\right)^2\right)_T - \left(\left(u_f - u_s\right)^2\right)_B\right]\left(\frac{u_f - u_s}{\mathbf{u_r}}\right) - \rho V C_m \frac{dv_s}{dt} - V(\rho_s - \rho)g. \tag{30}$$

7. Initial Conditions and Collisions with the Bed

7.1. Initial Conditions

There are a few approaches to formulating the initial conditions. Nino and Garcia (1994) estimated the initial conditions from the measurements of the trajectories of individual saltating particles obtained in special measurements [występuje tu chyba niepotrzebne powtórzenie "from the measurements … obtained in special measurements"]. These conditions consist of the values of normal and streamwise components of the particle velocity at the beginning of saltation.

Wilberg and Smith (1985) developed special equations from a theoretical point of view. They analyzed the critical balance between the drag force (acting parallel to the bed), the lift force (acting normal to the bed) and the gravitational force (acting in the vertical ["vertical plane" lub "vertical direction"]). Their analysis of the initial conditions is based on a bed configuration. They considered nonspherical sediment particles, but the critical shear stress and drag coefficients were calculated for spheres of equivalent volume. Eventually, after introducing some simplifying assumptions, they developed equations for the vertical and horizontal components of the particle velocity vector.

Van Rijn (1984) assumed that the initial position of the particle is 0.6 D over the bed surface, the initial horizontal and vertical velocities are equal to $2U_{*c}$, and the flow velocity distribution over the depth is described by the logarithmic law. He assumed that the drag force acts in the direction of the relative velocity, and the lift force in the perpendicular direction. In this paper Van Rijn's approach is used with some modifications.

8. Collisions at the Bed (Splash Function)

8.1. Post-Collision Velocities

Post-collision velocities in the case of particles sliding during collision are easy to calcula te by substituting the components of the impulse force Eqs. (19) and (20) into impulse equations (15). The two post-collision velocities are thus obtained as

$$\mathbf{v}_1 = \mathbf{v}_1^0 - (\mathbf{n} - f\mathbf{t})\left(\mathbf{n}\,\mathbf{V}^0\right)(1+e)\frac{m_2}{(m_1+m_2)}, \tag{31}$$

$$\mathbf{v}_2 = \mathbf{v}_2^0 + (\mathbf{n} - -f\mathbf{t})\left(\mathbf{n}\,\mathbf{V}^0\right)(1+e)\frac{m_1}{(m_1+m_2)}, \tag{32}$$

where $\mathbf{v}_1$ and $\mathbf{v}_2$ are the post-collision velocities of particles 1 and 2, respectively. Post-collision velocities in the case of particle-wall interaction are easy to obtain from Eqs. (23) and (24) by assuming that the bed is formed of uniformly packed spheres of the same size as transported particles. If the bed is not eroded, it is assumed that the mass of spheres forming the bed is much greater, say 500 times the mass of flowing particles. If the bed is much stronger, it is possible to assume that the particles forming the bed are much heavier.

Consider the case in which particle 1 falls with velocity $\mathbf{v}_1^0$ and collides with particle 2 located on the bed, i.e. $\mathrm{v}_2^0 = (0, 0)$. The possible range of the collision angle depends of the impact velocity vector and the geometry of the particle. For a spherical particle it equals (60°, 120°) (see Fig. 4). When the impact velocity vector is inclined to the horizontal axis at any angle from the range of (0°, 30°), it is easy to show that the minimum collision angle varies linearly with the impact angle, and the maximum collision angle can be calculated from the following formula (Rowiński and Czernuszenko 1999):

$$\tan\left(\alpha_{\max} - 90^\circ\right) = \frac{a\sqrt{1+a^2} + \sqrt{a(-a-2\sqrt{1+a^2})} + a^2}{a - a\sqrt{a(-a-2\sqrt{1+a^2})} + \sqrt{1+a^2}}, \tag{33}$$

where $\mathrm{a} = -\tan(\theta_{in})$ and $0 < \theta_{in} < 30$.

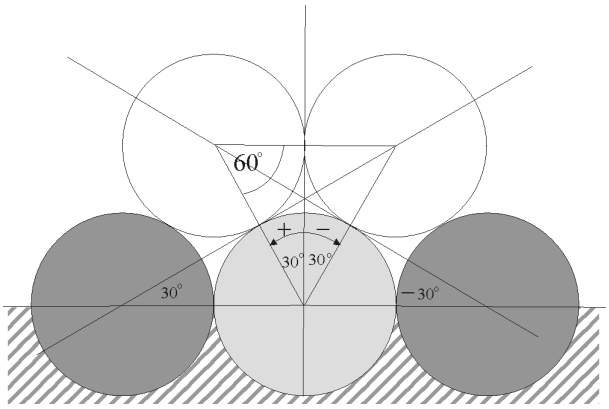

Fig. 4. The largest range of collision angles for collisions between the falling particle (the white spheres represent two extreme locations) and the bed particle (the light grey sphere) is (60°, 120°) for the incidence angle θ_{in} from the range of (30°, 90°). If θ_{in} is from the range of (0°, 30°), the range of possible collision angles is much smaller because of the two neighboring dark grey spheres

All possible ranges of collision and incidence angles are displayed in Figure 5. Since the collision angle is impossible to predict, a stochastic model proposed by Nino and Garcia (1994) is used to determine the probability distribution of alpha (the

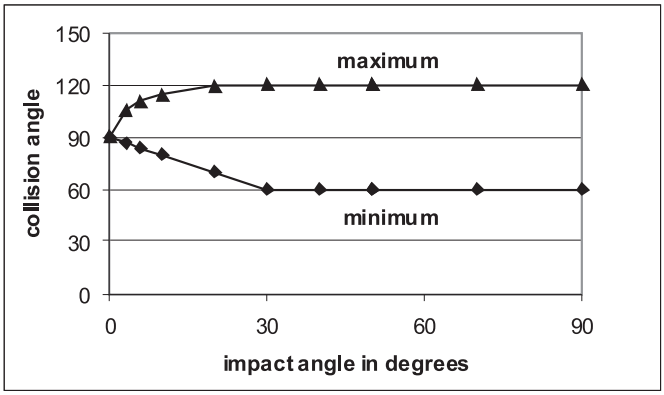

Fig. 5. Maximum and minimum collision angles (in degrees) as a function of impact angles. All angles are in degrees. [ta informacja jest już chyba w poprzednim zdaniu]

so-called the splash function). The conditional probability density function $p(\alpha|\theta_{in})$ is assumed to be uniform, which is equivalent to assuming that the particle has a uniform probability of being located anywhere in the bed. For a given incidental (impact) angle, the range of collision angles is determined from Figure 5, and the collision angle is determined with the use of a random number generator. Having determined the collision angle, one calculates the rebound velocity from Eq. (23) (or from Fig. 6) and defines the initial condition for the next saltation, i.e. the initial velocity.

Post-collision velocities can be calculated from Eqs. (23) and (24). The results of the calculations of the post-collision velocities of particle 1 falling with velocity $\mathbf{v}_1^0 = (0.707, -0.707)$ cm/s and striking the bed particle at $f = 0$ and $e = 0$ (perfect collision) and with coefficients $f = 0.4$ and $e = 0.6$ are presented in Figure 6. One can observe the role of restitution and friction coefficients for different collision angles between the flowing sediment particle and the particle on the bed.

Figure 6 shows the case in which the bed comprises uniformly packed spherical particles, and the flowing particle cannot strike the bed particle at a collision angle smaller than 60° or greater than 120° because of the adjoining (neighboring) particles (see the dark grey spheres in Fig. 4). The maximum of post-collision velocities for both components [a może "The maximum values for both components of the post-collision velocity"] of the bed particle are less than 0.002 cm/s, and they are not shown in the figure.

The horizontal as well as vertical components of the post-collision velocity should be positive to be certain continuous saltating process then the range of collision angle is shrunk [Nie rozumiem tego fragmentu.Może "to ensure continuous saltation. Then the range of collision shrinks"] to (65°, 112°) for a perfect collision and to (70°, 100°) for a collision with ($f = 0.4$, $e = 0.6$) (to read more about the continuous saltation process, see Lee, H.-Y. et al (2006), also Lee H-Y. et al (2000)). This shrinking depends on the friction and restitution coefficients (see Fig. 6).

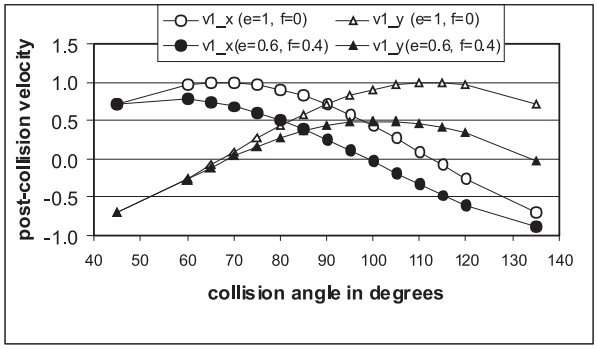

Fig. 6. Rebound velocity (after one hop) for the impact velocity $(1/\sqrt{2}, -1/\sqrt{2})$ as a function of the collision angle (the location of the bed grain) for the ideal collision ($e = 1$, $f = 0$) and the collision ($e = 0.6$, $f = 0.4$) assuming a very large $m2/m1$ ratio. Note the units: post-collision velocities have the same units as the given initial velocities (usually they are mm/s or cm/s)

9. Numerical Simulation Results

9.1. Model Verification

Data for the verification of our model was taken data of Lee & Hsu (1994), who conducted comprehensive measurements in a 12 m long, 0.3 m wide slope-adjustable recirculating flume. Several combinations of water depth, channel slope and particle size were tested. The range of water depth was from 3.71cm to 12.08 cm, and the rage of slope was from 0.0002 to 0.023. The effective roughness of the bed surface was about 1.36 mm. Two particle sizes were used, with the mean diameters of 1.36 mm and 2.47 mm. Specific gravity was 2.64. The flow was turbulent with the Reynolds number between 21000 and 73000, and the roughness Reynolds number varied from 50 to 146.

A real time flow visualization technique was applied in the study to investigate particle saltation near the channel bed. By this technique, particle trajectories and velocities were measured without disturbing the flow field (for more details see Lee & Hsu 1994).

Figures 7 and 8 show the result of a comparison of our results with the data of Lee & Hsu (1994).

It is easy to see from Figures 9 a-b that for large particles the length and the height of hops are smaller than for small particles.

10. Influences of Different Forces on the Particle Trajectory

The analysis is related only to the vertical components of all forces without F_{pc} because of the lack of specific data related to this force. The equation (22) can be rewritten in the following symbolic form:

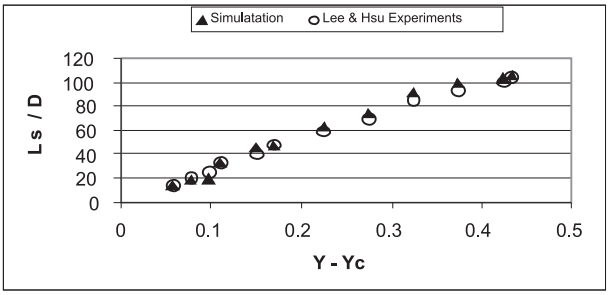

Fig. 7. Relation between simulated and experimental saltation length for Lee & Hsu (1994) data (taken from Bialik, 2010)

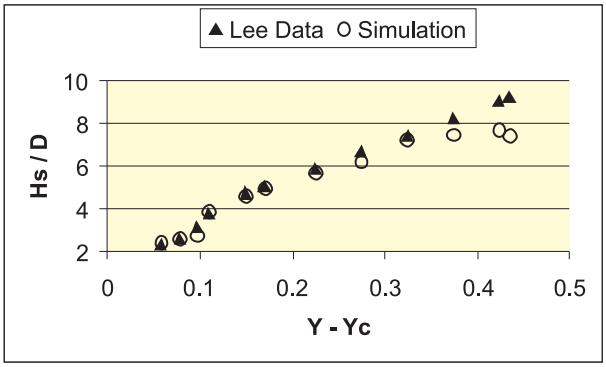

Fig. 8. Relation between simulated and experimental saltation length for Lee & Hsu (1994) data (taken from Bialik, 2010)

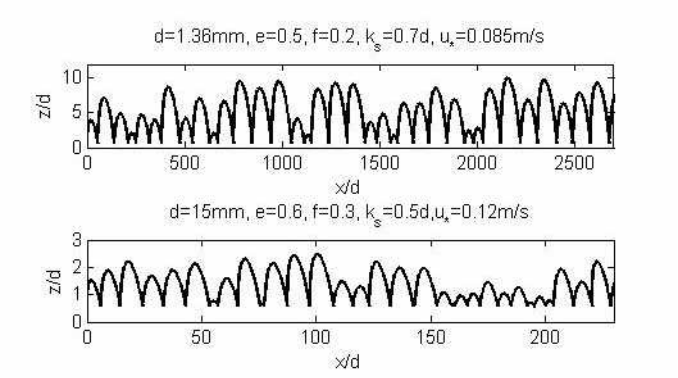

Fig. 9. A typical series of hops generated by the model for two particle diameters and two different flow conditions (taken from R. Bialik (2010))

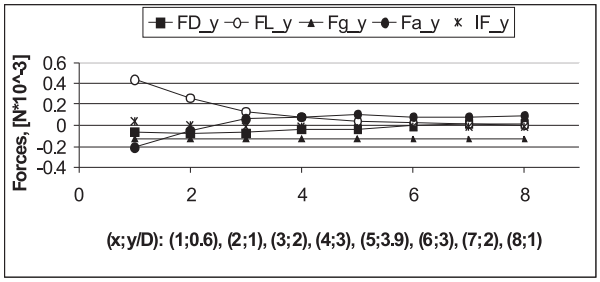

Fig. 10. Forces (in $N \times 10^{-3}$) exerted on a single particle during one hop (Run 4: $D = 2.47$ mm, $H = 4.64$ cm, $U = 1.125$ m/s, specific weight $\rho_s = 2.64$ g/cm^3, $U* = 0.075$ m/s, $k_e = 1.235$ mm). The location of the moving particle is $(x; y/D)$, where x is a (longitudinal) coordinate. The initial position of the particle is $x = 1$, and $x = 2, 3, \ldots$ are its successive positions in sequence. To re-calculate it in distance $-x'(x, y/D) = u(y/D) * (x - 1) * \Delta t(10^{-2})$, where y/D is a non-dimensional vertical coordinate. Points 1-5 represent the upward movement of the particle, points 6–8 represent its downward movement. C_m = virtual mass coefficient (assumed to be 0.50)

$$IF = F_a + FD + FL + F_g. \tag{34}$$

The time course of these forces during one hop is presented in Figure 10. The longitudinal coordinate it is easy to get if he knows the increment of time and velocities at selected distances from the bed. In this case these are $\Delta T = 0.01$ sec, and $y = 0.6D, 1D, 2D, 3D$, and $3.9D$.

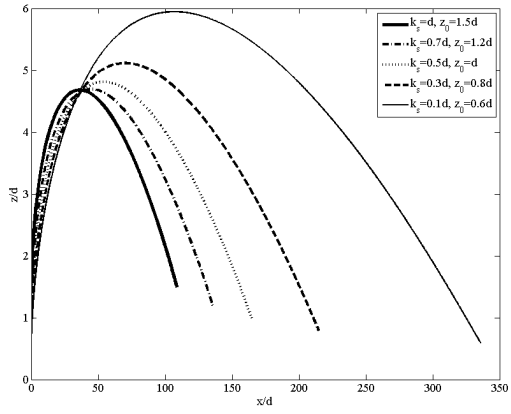

Fig. 11. Trajectories of the first hop for different roughness heights h_s and, in consequence, for different initial particle positions z_0 for the relative velocity $u(0) = v(0) = 2\ U_*$

The velocities can be calculated from Eq. (14). Figure 10 shows that at $x = 3$ (i.e., $2 \times \Delta t$) the particle begins to move slowly (with negative acceleration), but it still rises

until $x = 5$ (i.e. $4 \times \Delta t$), where the added mass force reaches its maximum. It is easy to calculate that at $x = 8$ the distance from the beginning of the movement is almost $33D$. The lift force is significantly greater than the drag force. Similar results were also obtained by Lee & Hsu (1994).

11. Influence of Roughness Height

The influence of the roughness height k_s on the first particle trajectory, i.e. on the longitudinal velocity of the particle for the initial velocity $u(0) = v(0) = 2\ U_*$ is displayed in Figure 11. The size of the particle is the same for all cases. It is easy to see that for the smallest k_s the trajectory is the highest and longest. In this case the particle is initially located in the largest velocity gradient, i.e. the lift force is the largest for the smallest roughness.

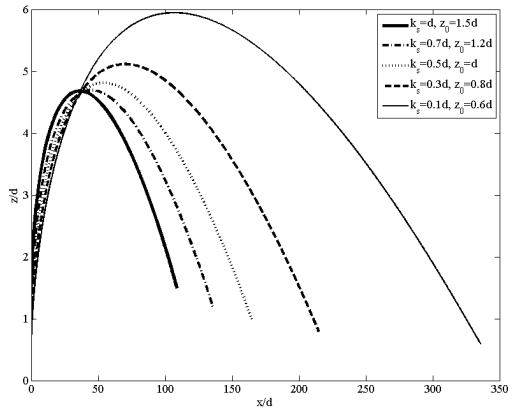

Fig. 12. Trajectories of the first hop for different roughness heights h_s and, in consequence, for different initial particle positions z_0 for the relative velocity $u(0) = v(0) = 2\ U_*$

12. Conclusions

1. The Lagrange model presented here produces trajectories of a single particle that are quite correct according to measurements. The model was calibrated and verified with experimental data. However, the model needs some calibration related to friction and restitution coefficients.
2. The boundary conditions assume that the initial distance of the particle center from the channel bed is 0.5 the diameter of the grain. The initial vertical and longitudinal particle velocities are estimated as approximately $2U_*$.
3. The roughness height has a strong influence on the lift force very close to the bed, especially for small roughness. In this case the lift forces greatly exceeded all other forces. This is due to direct effect on the gradient velocity distribution.

4. For large particles the length and height of hops are smaller than for small particles. The maximum saltation length and height in the present study were approximately 100D and 10D, respectively.
5. The lift force reaches its maximum value in the rising stage for the biggest difference between fluid and particle velocities, and then it gradually decreases almost to zero. The particle accelerates only for the first two time steps and then slows down (see Fig. 7).
6. The horizontal as well as vertical components of the post-collision velocity should be positive to ensure continuous saltation. Then the range of collision angles shrinks a little for a perfect collision and even more for a non-perfect collision. This shrinking depends on the friction and restitution coefficients.

Acknowledgments

This work was supported by grant N N306 658140 from The National Science Centre Grant, Poland. The author is grateful to Dr P. Rowinski for reviewing an early draft of the results and contributing helpful criticism. Also, he wishes to express his thanks to Dr R. Bialik for some calculations and drawing the pictures.

References

Auton T. R. (1987) The lift force on a spherical body in a rotational flow. *J. Fluid Mech.*, 183, 199–218.

Bagnold R. A. (1956) The flow of cohesionless grains in fluids, *Phil. Trans. R. Soc*. London A, 249, 235–297.

Bialik R. (2011) Particle-particle collision in Lagrangian modeling of saltating grains, *Journal of Hydraulic Research,* **49**(1), 23–31.

Bialik R. (2010) Modeling of saltating grains in river flows and transport of bed load sediment. Ph.D. Thesis (in Polish).

Coleman N. L. (1967) *A theoretical and experimental study of drag and lift forces acting on the sphere resting on a hypothetical streambed*, 12^{th} congress of the International Association for Hydraulic Research, Fort Collins, Colo.

Crowe C., Sommefeld M. and Tsuji Y. (1998) *Multiphase Flows with Droplets and Particles*, CRC Press, Boca Raton.

Czernuszenko W. (2007) *The logarithmic law for flows over large relative roughness*, 32nd Congress of IAHR, Venice, Italy, **1**, p. 372.

Czernuszenko W. (2009) Model of particle-particle interaction for saltating grains in water, *Archives of Hydro-Engineering and Environmental Mechanics*, 3–4.

Lee H-Y, Hsu I-S. (1994) Investigation of Saltating Particle Motions, *Journal of Hydraulic Eng*., 120 (4), 831–845.

Lee H.-Y., Lin Y.-T., You J.-Y., and Wang H.-W. (2006) On three-dimensional continuous saltating process of sediment particles near the channel bed, *Journal of Hydraulic Research,* **44**, (3), 374–389.

Lee H-Y. et al (2000) Investigations of continuous bed load saltating process, *Journal of Hydraulic Engineering*, 126(9), 691–99.

Nino Y. and Garcia M. H. (1996) Experiments on particle-turbulence interactions in the near-wall region of open channel flow, *Journal of Fluid Mechanics*, 326, 285–319.

Nino Y. and Garcia M. H. (1994) Gravel saltation, 2. Modeling, *Water Resources Research* 30(6), 1915–24.

Perry A. E., Schofield W. H., and Joubert P. N. (1969) Rough wall turbulent boundary layers, *Journal of Fluid Mechanics* 37, 383–413.

Rowiński P. M., Czernuszenko W. (1999) Modeling of sand grain paths in a turbulent open channel flow, *Proc. 28th IAHR Congress,* CD-ROM, Graz, Austria.

Schmeeckle M. W., Nelson J. M., Shreve R. L. (2007). Forces on stationary particle in near-bed turbulent flows, *Journal of Geophysical Research*, **112**, FD 2003, 1–23.

Sekine M. and Kikkawa H. (1992) Mechanics of saltating grains, II, *Journal of Hydraulic Engineering*, **118** (4), 536–538.

van Rijn L. C. (1987) *Mathematical Modeling of Morphological Processes,* Delft: Waterloopkundig Laboratorium.

Van Rijn, L. C. (1994) *Principles of Sediment Transport in Rivers, Estuaries and Coastal Seas*, AQUA Publications, Netherlands.

Wiberg P. L. and Smith J. D. (1985) A Theoretical Model for Saltating Grains in Water, *Journal of Geophysical Research* 90 (C4), 7341–7354.

Willets B. B., Naddch K. F. (1986) Measurements of lift on spheres fixed in low Reynolds number flows, *J. Hydraulic Res*., 24, 425–435.